Pannexin-1 and Ca V 1.1 show reciprocal interaction during excitation-contraction and excitation-transcription coupling in skeletal muscle

Francisco Jaque-Fernández, Gonzalo Jorquera, Jennifer Troc-Gajardo, France Pietri-Rouxel, Christel Gentil, Sonja Buvinic, Bruno Allard, Enrique Jaimovich, Vincent Jacquemond, Mariana Casas

Pannexin-1 and $Ca_V1.1$ show reciprocal interaction during excitation-contraction and excitation-transcription coupling in skeletal muscle

Francisco Jaque-Fernández[1], Gonzalo Jorquera[1,3], Jennifer Troc-Gajardo[1], France PietriRouxel[4], Christel Gentil[4], Sonja Buvinic[6] Bruno Allard[5], Enrique Jaimovich[1,2], Vincent Jacquemond[5] and Mariana Casas[1,2]

[1]Programa de Fisiología y Biofísica, ICBM, Facultad de Medicina, Universidad de Chile, Santiago, Chile

[2]Center for Exercise, Metabolism and Cancer, ICBM, Facultad de Medicina, Universidad de Chile, Santiago, Chile.

[3]Centro de Neurobiología y Fisiopatología Integrativa (CENFI), Instituto de Fisiología, Facultad de Ciencias, Universidad de Valparaíso, Chile.

[4]UPMC Université Paris 06/INSERM/CNRS/Institut de Myologie/Centre de Recherche en Myologie (CRM), GH Pitié Salpêtrière, Paris, France.

[5]Univ Lyon, Université Claude Bernard Lyon 1, CNRS UMR-5310, INSERM U-1217, Institut NeuroMyoGène, Lyon, France.

[6]Institute for Research in Dental Sciences, Faculty of Dentistry, Universidad de Chile, Santiago, Chile.

Running Title: $Ca_V1.1$-Pannexin interdependent-function in skeletal muscle

Corresponding author:

M. Casas, Programa de Fisiología y Biofísica Facultad de Medicina, Universidad de Chile Avda. Independencia 1027 838-0453, Santiago Chile Email: mcasas@med.uchile.cl

eTOC Summary

Jaque-Fernández et al. show that downregulation of $Ca_V1.1$ in muscle fibers elevates ATP release, whereas downregulation of Panx1 depresses depolarization-induced intracellular Ca^{2+} release. They conclude that Panx1 is a reciprocal partner of $Ca_V1.1$ for both E-C and E-T coupling.

Abstract

One of the most important functions of skeletal muscle is to respond to nerve stimuli by contracting. This function ensures body movement, but also participates in other important physiological roles, like regulation of glucose homeostasis. Muscle activity is closely regulated to adapt to different demands and shows a plasticity that relies on both transcriptional activity and nerve stimuli. These two processes, both dependent on depolarization of the plasma membrane, have so far been regarded as separated and independent processes, due to a lack of evidence of common protein partners or molecular mechanisms. In this study, we reveal intimate functional interactions between the process of excitation-induced contraction and the process of excitation-induced transcriptional activity in skeletal muscle. We show that the plasma membrane voltage-sensing protein $Ca_V1.1$ and the ATP releasing channel, Pannexin-1, regulate each other in a reciprocal manner, playing roles in both processes. Specifically, knockdown of $Ca_V1.1$ produces chronically elevated extracellular ATP concentrations at rest, consistent with disruption of the normal control of the Panx1 activity. Conversely, knockdown of Pannexin-1 not only affects activation of transcription but also affects $Ca_V1.1$ function on the control of muscle

fibers contraction. Altogether, our results establish the presence of bidirectional functional regulations between the molecular machineries involved in the control of contraction and of transcription induced by membrane depolarization of adult muscle fibers. Our results are important for an integrative understanding of skeletal muscle function and may have important impact for understanding several neuromuscular diseases.

Introduction

Besides its role in energy transfer, ATP is known to operate as an extracellular messenger for autocrine and paracrine signaling (Corriden and Insel 2010). Specifically, in a variety of cell types including muscle cells, ATP can be released across the plasma membrane into the extracellular medium through pannexin channels (D'Hondt et al. 2011). Pannexin-1 is an integral membrane glycoprotein that belongs to a family of proteins encoded by three genes in vertebrates (*Panx1*, *Panx2*, and *Panx3*). A widespread tissue distribution of Panx1 has been established, with highest levels found in skeletal muscle (Baranova et al. 2004).

Roles for Panx1 have been described in a variety of physiological and pathological processes including propagation of intercellular Ca^{2+} (Locovei et al. 2006), afferent neurotransmission (Romanov et al. 2007), activation of the inflammasome (Silverman et al. 2009), recruitment of macrophages to apoptotic cells (Chekeni et al. 2010), pressure overload-induced fibrosis in the heart (Nishida et al. 2008) and ionic dysregulation during stroke-induced ischemic neuronal death (Thompson et al. 2006). Panx1 has also been shown to contribute to epileptic-form seizure activity (Thompson et al. 2008). The opening of Panx1 channel is essential to its function and any deregulation leading to uncontrolled opening may cause cell death (Thompson et al. 2006). Thus, a robust mechanism controlling the opening and closure of Panx1 is of vital importance to the cells. Along with this line, Panx1 channels are known to be potentially activated by different stimuli like mechanical stress (Bao et al. 2004), elevation of intracellular [Ca^{2+}] (Locovei et al. 2006), activation of P2Y purinergic receptors (Locovei et al. 2006, Pelegrin and Surprenant 2006)

and ischemic or hypoxic conditions (Sridharan et al. 2010, Thompson et al. 2006). Despite the high level of expression of Panx1 in differentiated muscle, its role in this tissue has remained obscure until Panx1 was found to be involved in an interaction with the membrane protein $Ca_V1.1$ (Arias-Calderon et al. 2016, Jorquera et al. 2013).

$Ca_V1.1$ is the voltage sensor for skeletal muscle Excitation Contraction (EC) coupling. Upon membrane depolarization, it undergoes conformational changes that trigger the opening of Ryanodine Receptor 1 (RyR1) channels in the Sarcoplasmic Reticulum (SR) membrane, through protein-protein conformational coupling: this generates a rise in cytosolic [Ca^{2+}] that activates contraction (see (Rios and Pizarro 1991, Schneider 1994)). The coupling of Cav1.1 with RyR1 is a particular case because beyond the orthograde control that $Ca_V1.1$ exerts over RyR1 activity, there is also a retrograde control of $Ca_V1.1$ by RyR1 (Andronache et al. 2009, Bannister and Beam 2009, Esteve et al. 2010, Nakai et al. 1996). These two proteins interact physically and functionally to make the robust complex that ensures EC coupling (Beam and Bannister 2010, Paolini et al. 2004, Rebbeck et al. 2014, Rios and Brum 1987, Samso 2015).

$Ca_V1.1$ operates also as a voltage-gated Ca^{2+} channel responsible for a slow Ca^{2+} entry across the t-tubule membrane upon membrane depolarization (Rios and Pizarro 1991, Tanabe et al. 1990). Although not essential for EC coupling (Dayal et al. 2017), there is evidence that this Ca^{2+} entry contributes to refilling of the SR Ca^{2+} store (Lee et al. 2015, Robin and Allard 2015) and that it is also coupled to CaMKII activation with consequent impact on downstream signaling pathways affecting muscle metabolism (Georgiou et al. 2015, Lee et al. 2015).

A third role for $Ca_V1.1$ was demonstrated in recent years, as a trigger for activation of a frequency-dependent signaling cascade related to Excitation Transcription (ET) coupling, where $Ca_V1.1$ voltage-sensing activity is coupled to activation of ATP release out of the muscle cells through Panx1 channels after electrical stimulation (ES), in a frequency-dependent manner (Arias-Calderon et al. 2016, Buvinic et al. 2009, Jorquera et al. 2013). Released ATP binds purinergic receptors which activate a signaling cascade responsible for changes in the transcriptional activity of genes involved in muscle plasticity. Moreover, ES-dependent ATP release is practically absent in cultured muscle cells lacking $Ca_V1.1$, and the $Ca_V1.1$ blocker nifedipine completely abolishes both ATP release and transcriptional activity produced by a permissive frequency of ES in adult muscle fibers (Casas et al. 2014, Jorquera et al. 2013). It has been shown that Panx1 is in close proximity to several proteins related to ET coupling, including $Ca_V1.1$ (Arias-Calderon et al. 2016, Jorquera et al. 2013) and P2Y2 (Arias-Calderon et al. 2016).

In the past years, knock-down or expression of mutated forms of other proteins has been shown to affect either $Ca_V1.1$ membrane expression and/or functional features of $Ca_V1.1$, as EC coupling. Notably, it has been established that, besides $Ca_V1.1$ and RyR1, β1a, Stac3 and junctophilin-2 are necessary for activation of EC coupling in skeletal muscle (Couchoux et al. 2007, Golini et al. 2011, Mosca et al. 2013, Perni et al. 2017, Polster et al. 2016, Weiss et al. 2008). Other proteins can also modulate $Ca_V1.1$ activity, like Cav3, JP-45 and junctophilin-1, altering either or both, calcium current and activation of intracellular Ca^{2+} release (Anderson et al. 2006, Weiss et al. 2008).

In the present work, we propose that Panx1 belongs to the family of proteins that are

functional interacting partners of $Ca_V1.1$, affecting its role in ET and EC coupling. Indeed, a reduction of Panx1 alters $Ca_V1.1$ Ca^{2+} channel properties, compromises the EC coupling function and impairs transcriptional activation of target genes after low frequency electrical stimulation of fully differentiated muscle fibers. Moreover, we show that Panx1 and $Ca_V1.1$ may also be reciprocal partners capable of mutually regulating their respective function, because a reduction in $Ca_V1.1$ content alters Panx1 proper control of ATP release, consequently affecting transcriptional activity.

Materials and methods

Ethical approval

All experiments and procedures were conducted in accordance with the guidelines of the local animal ethics committee of the University of Chile, University Paris 06, University Claude Bernard Lyon 1, the French Ministry of Agriculture (decree 87/848) and the revised European Directive 2010/63/EU and conform to the principles and regulations as described in the Editorial by Grundy (2015).

Down-expression of Pannexin-1 in muscle fibers

AAV-mCherry-U6-mPANX1-shRNA plasmid was obtained from Vector Biolabs. It targets a specific sequence of mouse Panx1 and has been validated for ~90% knockdown of mRNA in B16-F0 cells.

Exogenous expression by electroporation was performed in the *flexor digitorum brevis* (*fdb*) muscles of 6-7-week-old either Swiss OF1 (charge movement measurements) or BalbC (Ca^{2+} current and Ca^{2+} release measurements) male mice using a general

procedure previously described (Legrand et al. 2008). Mice were anaesthetized either by isoflurane inhalation (3% in air, 300 ml.min^{-1}) using a commercial delivery system (Univentor 400 Anaesthesia Unit, Uninventor, Zejtun, Malta) or by intraperitoneal injection of a mix of 0.1 g/kg ketamine and 0.01 g/kg xylazine. Twenty-five microliters of a solution containing 2 mg/ml hyaluronidase dissolved in sterile saline were then injected into the footpads of each hind paw. Forty minutes later the mouse was re-anaesthetized using the same procedure as for hyaluronidase injection. A 20 µL volume of Tyrode solution containing 1µg/µL mCherry DNA was injected into the footpad of a hind paw whereas the same volume of solution containing 1µg/µL shRNA-Panx1 DNA was injected into the footpad of the contralateral hind paw. Following the injections, two gold-plated stainless-steel acupuncture needles connected to the electroporation apparatus were inserted under the skin, near the proximal and distal portion of the foot, respectively. The standard protocol used consisted in 20 pulses of 100 V/cm amplitude and 20 ms duration delivered at a frequency of 1 Hz by a BTX ECM 830 square wave pulse generator (Harvard Apparatus, Holliston, USA). Experimental observations and measurements were carried out 2 weeks later. Fibers positive for mCherry that were isolated from muscles transfected with shRNA-Panx1 and from muscles transfected with solely mCherry are referred to as shRNA-Panx1 and corresponding control fibers, respectively.

Down-expression of $Ca_V1.1$ in muscle fibers

Down expression of α1s subunit of DHPR was achieved by a U7-exon skipping strategy using adenovirus-associated viral vectors (AAV-U7delα1s). Previously designed antisense sequence and control non-functional construct were used as described earlier

(Pietri-Rouxel et al. 2010). In brief, adult C57/Black6 mice were anaesthetized with a mix of 0.1 g/kg ketamine and 0.01 g/kg xylazine. Two intramuscular injections in 24 h of a mixture containing AAV (U7-SA) and AAV (U7-ESE) were carried out in one footpad and the contra-lateral footpad was injected with the control AAV (U7-Ctrl). Experimental measurements were carried out 4 months later. Fibers isolated from muscles treated with the active AAV and with the non-functional construct are referred to as ΔDHPR and corresponding control fibers as WT, respectively.

Preparation of isolated muscle fibers for electrophysiology and Ca^{2+} measurements

Single fibers were isolated from the *flexor digitorium brevis* (fdb*)* muscles using a previously described procedure (Jacquemond 1997). In brief, mice were euthhanized by cervical dislocation before removal of the muscles. Muscles were treated with collagenase (Sigma, type 1) for 60 min at 37°C. Single fibers were then obtained by dissociating the muscles within the experimental chamber. Fibers were dispersed on the glass bottom of a 50 mm wide culture μ-dish (Ibidi, München, Germany). Fibers were first partially insulated with silicone grease, as described previously (Jacquemond 1997) so that only a portion of the fiber extremity was left out of the silicone. All experiments were performed at room temperature (20-22 °C).

Extracellular ATP measurement

50 μL of extracellular media aliquots from fibers plates were removed at different times. ATP concentrations were measured with the CellTiter-Glo® Luminescent Cell Viability Assay (Promega, Madison, WI, USA), as reported (Jorquera et al. 2013). Data were

calculated as pmol extracellular ATP/μg total RNA and the ratios between experimental versus control points were reported. Normalization by total RNA instead of total protein was chosen because adult muscle fibers were seeded on a matrigel coated surface (containing a large amount of protein), which may affect the protein determination associated to fibers only. Total RNA was obtained from skeletal muscle fibers employing Trizol reagent (Invitrogen, Corp., Carlsbad, CA, USA) according to manufacturer's protocol.

Real time PCR

Total RNA was obtained from skeletal muscle fibers employing Trizol reagent (Invitrogen, Corp., Carlsbad, CA, USA) according to manufacturer's protocol. cDNA was prepared from 1 μg of RNA, using SuperScript II enzyme (Invitrogen), according to manufacturer's protocol. Real-time PCR was performed using Stratagene Mx3000P (Stratagene, La Jolla, CA, USA) using the Brilliant III Ultra-Fast QPCR & QRT-PCR Master Mix amplification kit (Agilent Technologies, Santa Clara, CA, USA). The primers used were: TnIs: 5'-GAGGTTGTGGGCTTGCTGTATGA-3' (sense), 5'-GGAGCGCATATTAGGGATGT-3' (antisense); TnIf: 5'-AGGTGAAGGTGCAGAAGAGC-3' (sense), 5'-TTGCCCCTCAGGTCAAATAG-3'(antisense); β-actin:5'-TACAATGAGCTGCGTGTG-3' (sense), 5'-TACATGGCTGGGGTGTTGAA-3' (antisense), P0: 5'-CTCCAAGCAGATGCAGCAGA-3' (sense), 5'-ATAGCCTTGCGCATCATGGT-3' (antisense). All primers used presented optimal amplification efficiency (between 90% and 110%). PCR amplification of the housekeeping gene β-actin or P0 was performed as control. Thermocycling conditions were as follow: 95°C for 3 min and 40 cycles of 95°C for 10 s, 60°C for 20 s. Expression values were normalized to β-actin or P0 and reported in

units of $2^{-\Delta\Delta CT}$ ± SEM. CT value was determined by MXPro software when fluorescence was 25% higher than background. PCR products were verified by melting-curve analysis.

*We**stern Blot Analysis***

Muscles were lysed in 60 μL of ice-cold lysis buffer (20 mM Tris-HCl, pH 7.4, 1% Triton X-100, 2 mM EDTA, 10 mM Na_3VO_4, 20 mM NaF, 10 mM sodium pyrophosphate, 150 mM NaCl, 1 mM PMSF and a protease inhibitor mixture). 30 μg of total protein from cell lysates were separated in 10% SDS-polyacrylamide gels and transferred to polyvinylidenedifluoride membranes (Millipore). Membranes were blocked at room temperature for 1 h in Tris-buffered Saline containing 3% fat-free milk, with or without 0.5% Tween 20, and then incubated overnight with the appropriate primary antibody. For Cav1.1, a mouse monoclonal antibody (1:2.000) from Abcam (ab2862) was used (Hu et al. 2015) (Hu *et al.*, 2015). For Panx-1, a rabbit polyclonal antibody (1:10.000) from Thermo Fisher Scientific (N°Cat: 487900) was used (Melhorn et al. 2013). alpha-actin (1:1000) from Sigma-Aldrich (a2066) (Mormeneo et al. 2012) or β-tubulin from Cell Signaling (11H10) (Gallot et al. 2017) were used as charge control for normalization of different lanes.

Membranes were incubated with the appropriate secondary antibody at room temperature for 1.5 h. The immunoreactive proteins were detected using ECL reagents according to the manufacturer's instructions. For loading control, membranes were stripped in buffer containing 0.2 M Glycine (pH 2) and 0.05% Tween 20, at room temperature for 30 min, blocked as previously, and assessed with the corresponding control antibody.

Electrophysiology

Whole-cell voltage-clamp experiments were performed: for measurements of DHPR Ca^{2+} current and intracellular Ca^{2+} transients in fibers expressing shRNA-Pnx1 and/or mCherry, an Axopatch 200B patch-clamp amplifier (Molecular Devices, Sunnyvale, CA) was used and data acquisition and command voltage pulse generation was achieved with a Digidata 1322A analog-digital, digital-analog converter (Axon Instruments, Foster City, CA) controlled by pClamp software (Axon Instruments). For measurements of DHPR Ca^{2+} current in fibers down-expressing CaV1.1, an RK-400 patch-clamp amplifier (Bio-Logic, Claix, France) was used in combination with a Digidata 1322A converter (Axon Instruments) controlled by pClamp software (Axon Instruments). For measurements of intracellular Ca^{2+} transients in fibers down-expressing CaV1.1 and for measurements of intramembrane charge movement in fibers expressing shRNA-Pnx1 and/or mCherry, an RK-400 patch-clamp amplifier (Bio-Logic, Claix, France) was used in combination with a BNC-2120 converter (National Instruments, Austin, TX) controlled by WinWCP software (University of Strathclyde, Glasgow, UK). Fibers were bathed in a TEA-containing extracellular solution (see Solutions). Voltage-clamp was performed with a micropipette filled with the intracellular-like solution (see Solutions). The tip of the micropipette was inserted through the silicone within the insulated part of the fiber and it was slightly crushed against the bottom of the chamber in order to decrease the access resistance. Analog compensation was adjusted to further decrease the effective series resistance. Membrane depolarizing steps were applied from a holding command potential of -80 mV. The Cav1.1 Ca^{2+} current was measured in response to 0.5 s-long depolarizing steps of increasing level. The linear leak component of the current was removed by subtracting the

adequately scaled value of the steady current measured during a 20 mV hyperpolarizing step. Peak current values were normalized by the fiber capacitance. The voltage dependence of the peak current was fitted with the following equation:

$$I(V) = Gmax(V-Vrev)/(1+\exp(V0.5-V)/k]) \quad (1)$$

with *I(V)* the peak current density at the command voltage *V*, *Gmax* the maximum conductance, *Vrev* the apparent reversal potential, *V0.5* the half-activation potential and *k* the steepness factor. It should be stressed that Ca^{2+} current measurements designed to test the consequences of Pannexin-1 down expression and of CaV1.1 down-expression, respectively, were performed on muscle fibers from mice of different strains and age and under slightly differing conditions which explain the difference in current density between the two data groups.

Intramembrane charge movement currents were measured and analyzed according to previously described procedures (Collet et al. 2003, Pouvreau et al. 2004). In brief, adequately scaled control current records elicited by 50 ms-long hyperpolarizing pulses of 20 mV were subtracted from the current elicited by test depolarizing pulses of the same duration to various levels. In a few cases, test records were further corrected for a sloping baseline using previously described procedures (Horowicz and Schneider 1981). The amount of charge moved during a test pulse was measured by integrating the *on* and *off a* portion of the corrected test current records. The calculated charge was normalized to the capacitance of the fiber. The steady-state distribution of the normalized charge was fitted with a two-state Boltzmann function: $Q(V)=Qmax/(1+\exp[(V0.5-V)/k]) \quad (2)$

Qmax corresponding to the maximally available charge, *V0.5* to the voltage of equal charge distribution and *k* to the steepness factor.

Intracellular Ca^{2+} measurements

Voltage-activated Ca^{2+} transients in fibers expressing shRNA-Panx1 and/or mCherry were measured with the dye fluo-4: for this, muscle fibers were equilibrated for 30 minutes in the presence of 10 μM fluo-4 AM prior to establishing the silicone voltage-clamp conditions. Fluo-4 Ca^{2+} transients were measured with the line-scan mode (1.53 ms per line) of a Zeiss LSM 710 confocal microscope. The dye was excited with the 488 nm line of the argon laser and a 505-530 nm band pass filter was used on the detection channel. Fluo-4 Ca^{2+} transients were expressed as F/F0 where F0 is the background corrected baseline fluorescence.

Voltage-activated Ca^{2+} transients in fibers down-expressing CaV1.1 and corresponding control fibers were measured with the dye indo-1 following previously described procedures (Pouvreau et al. 2004, Weiss et al. 2010). In brief, prior to voltage clamp, the Ca^{2+} sensitive dye indo-1 was introduced locally into the fiber by pressure microinjection through a micropipette containing 1 mM indo-1 dissolved in the intracellular-like solution (see Solutions). Fibers were then left for 1 h to allow for intracellular equilibration. Indo-1 fluorescence was measured on an inverted Nikon Diaphot epifluorescence microscope equipped with a commercial optical system allowing simultaneous detection of fluorescence at 405 nm (F405) and 485 nm (F485) by two photomultipliers (IonOptix, Milton, MA, USA), upon excitation at 360 nm. The standard ratio method was used to calculate $[Ca^{2+}]$ from R=F405/F485, with *in vivo* values for the calibration parameters Rmin, Rmax, KD and β determined as previously described (Jacquemond 1997).

This same set-up and related procedures were also used to estimate the SR Ca^{2+} content in fibers expressing shRNA-Panx1 and/or mCherry using a method described by Al Qusairi et al., (2009). For this, muscle fibers were equilibrated for 30 minutes with the voltage-clamp pipette intracellular-like solution also containing indo-1 and EGTA (see Solutions). Then, 50-ms-long depolarizing pulses from -80 to +10 mV were applied, before and after applying 50 μM cyclopiazonic acid (CPA) in the extracellular medium, using a thin polyethylene capillary perfusion system operating by gravity. The maximum change in baseline indo-1 saturation level following pulses delivered in the presence of CPA was taken as an index of the SR Ca^{2+} content.

Solutions

The standard intracellular-like solution used in the voltage-clamp pipette contained (in mM) 140 K-glutamate, 5 Na2-ATP, 5 Na2-phosphocreatine, 5.5 MgCl2, 5 glucose, 5 HEPES. For $Ca_V1.1$ Ca^{2+} current measurements in fibers expressing shRNA-Panx1 and/or mCherry, this solution also contained 20 mM EGTA. For the experiments aimed at estimating the SR Ca^{2+} content in fibers expressing shRNA-Panx1 and/or mCherry, the standard intracellular-like solution also contained containing 0.2 mM indo-1, 20 mM EGTA and 8 mM CaCl2. For intramembrane charge movement, the intra-pipette solution contained 140 TEA-methanesulfonate, 5 Na2-ATP, 5 Na2-phosphocreatine, 5.5 MgCl2, 5 glucose, 20 EGTA, 5 HEPES.

The standard extracellular solution contained (in mM) 140 TEA-methanesulfonate, 2.5 CaCl2, 2 MgCl2, 1 4-aminopyridine, 10 TEA-HEPES and 0.002 tetrodotoxin. For CaV1.1 Ca^{2+} current measurements in fibers down-expressing CaV1.1 and corresponding

control fibers, the standard solution also contained EGTA-AM (5 μM). For Ca^{2+} measurements with fluo-4, 50 μM N-benzyl-p-toluene sulphonamide (BTS) was added to the standard solution. For intramembrane charge movement the extracellular solution contained 140 TEA-methanesulfonate, 0.1 CaCl2, 1 MnCl2, 1 CdCl2, 1 4-aminopyridine, 10 TEA-HEPES and 0.002 tetrodotoxin. All solutions were adjusted to pH 7.20.

Statistics

Statistical analysis was performed using Microcal Origin, version 8.0 (OriginLab Corp., Northampton, MA, USA) and GraphPad Prism 9. Least-squares fits were performed using a Marquardt-Levenberg algorithm routine included in Microcal Origin. Data values are presented as means ± S.E.M., for N number of animals. Statistical differences were determined assuming significance for $P < 0.05$ (*/$^{\neq}$ $P < 0.05$, **/$^{\neq\neq}$ $P < 0.01$, *** $P < 0.005$, **** $P < 0.001$). If groups followed a normal distribution a Student's t-test was applied. When, even normally distributed, they do not have the same SD, the t-test were followed by a Welch's correction. When data were not normally distributed, Kruskal-Wallis o Mann-Whitney test were applied. For the case of electrophysiological measurement, we performed a nested analysis of the data following instruction given in Eisner, 2021, where N was the number of animals, and n number of fibers form each animal. Numbers of individual measurement and individual animals used are mentioned in figure legends.

Results

Down-expression of $Ca_V1.1$ in adult muscle fibers alters the function of Pannexin-1

We have described that ATP release through Panx1 is activated by $Ca_V1.1$ at low frequencies of electrical stimulation in adult muscle fibers (Casas et al. 2010, Jorquera et al. 2013). To study a possible change in Panx1 activity induced by the loss of CaV1.1 in adult muscle, we used a model of down-expression of CaV1.1 taking advantage of a U7-exon skipping strategy (Pietri-Rouxel et al. 2010). In these muscles (ΔDHPR), we observed a reduction of 60% in protein levels of $Ca_V1.1$ (Fig. 1A). Importantly, in these fibers down-expressing $Ca_V1.1$, we observed increased basal levels of ATP release (Fig. 1B), indicating a deregulation of the normally closed configuration of Panx1 channel in resting conditions. After electrical stimulation, ΔDHPR fibers did not show an increase in extracellular ATP levels compared to control fibers (Fig. 1B). An extreme example of the absence of $Ca_V1.1$ is the mdg muscle cell, originally obtained from dysgenic mice not expressing $Ca_V1.1$. These cells showed to have increased values of basal ATP release compared to wild type myotubes and this release was inhibited by incubation with 5μM carbenoxolone (Fig 1C), indicating that ATP release occurs via Panx1 channels. Accordingly, in ΔDHPR fibers, the maintained increase in basal extracellular ATP levels, induced an increase in mRNA levels of the slow isoform of Troponin I (TnIs) and a decrease in mRNA levels of the fast isoform of this gene (TnIf) (Fig. 1D), a phenomenon previously seen in fibers stimulated with 20 Hz electrical stimulation (ES) or in fibers exposed to 30 μM external ATP (Jorquera et al. 2013). It is important to mention that 4 h after electrical stimulation, ΔDHPR fibers did not show changes in mRNA levels of TnI isoforms compared to not stimulated fibers (Fig. 1D).

To check the functional consequences of $Ca_V1.1$ down-expression, voltage-activated Ca^{2+} current and cytosolic Ca^{2+} transients were measured in a separate set of muscle fibers from control and U7-exon treated muscles, 4 months following AAV

transduction. Figure 2A shows representative Ca^{2+} current traces from a control fiber and from a U7-exon skipped fiber. Figure 2B shows the mean values for peak Ca^{2+} current density *versus* voltage in the two populations of fibers. Fitting the individual series of data points in each fiber with equation 1 gave mean values for *Gmax, Vrev*, *V0.5* and *k* of 234 ± 19 S/F, 68 ± 2 mV, 5 ± 1 mV, 6 ± 0.4 mV, and 166 ± 14 S/F, 69 ± 3 mV, 3 ± 1 mV, 5 ± 0.4 mV, in control (n=14, from N=4 mice) and U7-exon skipped fibers (n=14, from N=4 mice), respectively (Fig. 2B, right panel). There was a significant ~30 % reduction in the maximal conductance in the U7-exon skipped fibers. For this significant variation (Gmax), we made a Nested analysis that conclude the same significant difference in Gmax between two groups. The left panel in Figure 2C shows indo-1 Ca^{2+} transients from a control fiber and from a U7-exon skipped fiber obtained in response to depolarizing pulses from -80 to +10 mV of 20 ms duration. Resting [Ca^{2+}] level did not differ between the two groups of fibers (Fig. 2C, right). Also, fitting a single exponential function to the decay of the Ca^{2+} transients showed no significant difference in the mean values between control and U7-exon skipped fibers, suggesting that the Ca^{2+} removal capabilities of the fibers were unaffected (mean τ values were 48.2 ± 9 and 49.5 ± 13 ms in control and U7-exon treated fibers, respectively). Conversely, the peak [Ca^{2+}] level reached in response to a depolarizing pulse was significantly depressed in the U7exon skipped fibers, by 34 % (Fig. 2C, right). Same as above, for this significantly different set of data, we made a Nested analysis that conclude the existence of the same significant difference in peak [Ca^{2+}] level between two groups. Altogether, these results establish a significant alteration of the Ca^{2+} channel and EC coupling activity of $Ca_V1.1$ in fibers treated with the active AAV. The fact

that the relative depression in Ca^{2+} current density was lower than the decrease in protein level (Fig. 1A) was likely due to the use of different preparations of AAV in the two sets of experiments.

Down-expression of Pannexin-1 suppresses low frequency electrical stimulation-induced ATP release in adult muscle fibers

We first performed experiments to validate the Panx1 knock-down model. For this aim, we electroporated the AAV-mCherry-U6-mPANX1-shRNA plasmid (shPanx1) in the *fdb* muscles of mice. To distinguish the effects of Panx1 down-expression from possible consequences of electroporation and overexpression of a fluorescent protein, we electroporated a mCherry carrying plasmid in the muscle from the contralateral paw to use the corresponding fibers as controls. We waited for two weeks to evaluate levels of expression of Panx1 and the consequent disturbance of ATP release induced after electrical stimulation (ES) of fibers at 20 Hz (Jorquera et al. 2013). In Fig. 3A we show the expression of the mCherry reporter in muscles electroporated with the shPanx1 (carrying mCherry marker) and mCherry (alone) plasmid. We observed a broad level of fluorescence in *fdb* muscle indicating expression of the fluorescent protein. Results in Fig. 3B (representative Western blot and quantification of protein levels from 3 different preparations) show that Panx1 protein level had dropped by about 65% in muscles electroporated with the shPanx1 plasmid. This reduction in protein levels correlates with changes in ATP release in those fibers: in basal condition, extracellular ATP levels were significantly lower in shPanx1 expressing fibers compared with control ones (Fig. 3C upper graph). Importantly, the high levels of ATP release observed after 20 Hz ES (Jorquera et al.

2013) were clearly reduced in shPanx1 expressing fibers (Fig. 3C lower graph). After 20 Hz ES of control muscle fibers, there is an increase in mRNA levels of slow isoform of Troponin I (TnIs) and a decrease in mRNA levels of the fast isoform (TnIf) (Fig. 3 D) as previously published (Jorquera et al. 2013). Nevertheless, in fibers electroporated with the shPanx1 plasmid, the electrical stimuli failed to induce these transcriptional changes. There appears to be a reduction of basal levels of TnIs in shPanx1 compared to control, but it reaches no statistical difference (98±5.5 in controls vs 54±15.7 in shPanx 1 fibers, p=0.1).

Down-expression of Pannexin-1 does not alter Ca^{2+} current trough $Ca_V1.1$

We previously showed that pharmacological alteration of $Ca_V1.1$ activity is associated with an altered Panx1 function (Jorquera et al. 2013). In the present work, we looked for a possible involvement of Panx1 over $Ca_V1.1$ function. We first examined the Ca^{2+} channel activity of $Ca_V1.1$ in voltage clamped fibers down-expressing Panx1, while mCherry expressing fibers were used as control, as described in Methods section. Mean values for the capacitance in the mCherry and in the shPanx1 groups of fibers in these experiments were 1.02 ± 0.14 (22 fibers form 5 different animals) and 1.22 ± 0.08 nF (21 fibers form 4 different animals), respectively, statistically not different. Regarding the access resistance, as explained in the Methods section, its value is minimized by crushing the tip of the voltage-clamp micropipette once it is inserted in the silicone-embedded portion of muscle fiber. In order to test for a possible difference in voltage-clamp kinetics between the two groups of fibers we fitted the decay of the capacitive transient elicited by a 20 mV hyperpolarizing voltage step with a double-exponential function. Mean values for the fast and slow time constants in the mCherry and in the shPanx1 groups were 0.77 ±

0.14 and 0.57 ± 0.09 ms, and 2.52 ± 0.22 and 3.14 ± 0.55 (22 fibers from 5 animals in control group, and 21 fibers from 4 different animals in the shPanx1 group), respectively, also not statistically different. Figure 4A shows Ca^{2+} current records from a control fiber and from a fiber transfected with the shPanx1 plasmid. Records were obtained in response to 0.5 s-long depolarizing pulses from -80 mV to levels ranging between -20 and +40 mV. The peak amplitude of the current was lower in the shPanx1 condition and the kinetics of the Ca^{2+} current also appeared slower. Figure 4B shows the mean peak current *versus* voltage relationship from measurements in 22 control fibers (from 5 different animals) and 21 fibers (from 4 different animals) expressing the shRNA against Panx1. Individual series of data points in each fiber were fitted with equation 1, mean corresponding values for the parameters are reported in Fig. 4C, showing a 27 % reduction in the maximal conductance in fibers expressing the shPanx1 as compared to mCherry expressing fibers, whereas other parameters were unchanged. As each animal was electroporated in one paw with mCherry expressing plasmid and its contralateral paw with the shPanx1plasmid, we may consider that each fiber (even when coming from the same animal) could be consider as an independent measure rather than considered as a replicant form other fibers measured coming from the same muscle. In this case, the reduction in maximal conductance is significant ($p=0.0274$). However, when compared using a Nested analysis, this difference shows to be not significant. There was no significant difference also between sub-columns of the same group. The spontaneous Ca^{2+} current decay during the large pulses also appeared slower in shPanx1 as compared to control fibers. As it was too slow to be fitted with a single exponential, we evaluated this parameter by counting the number of fibers yielding at least a half decrease of the peak current during the pulse to +20 mV. This

corresponded to 81 % and 33 % of the control and shPanx1 fibers, respectively. Altogether, down-expression of Panx1 did not produced significant alterations in $Ca_V1.1$ Ca^{2+} current properties. May be more experiment would be needed to increase N values to evaluate the difference in Gmax. The size of both control and shPanx1 fibers Ca^{2+} currents is smaller than that shown in Fig. 2. This is due to the fact that eight-month-old C57/Bl6 mice were used for experiments described in that figure as compared to 6-7 weeks-old BalbC mice in Fig.4.

Down-expression of Pannexin-1 depresses voltage-activated SR Ca^{2+} release

One critical function of the $Ca_V1.1$ protein is its role in EC coupling. We addressed the issue of whether RyR1-mediated SR Ca^{2+} release would be altered in this condition of Panx1 down-expression. Figure 5A shows representative fluo-4 Ca^{2+} transients elicited by a train of short depolarizing pulses of increasing amplitude in a control (mCherry) and in a shPanx1 muscle fiber. While the overall qualitative time course of change in Ca^{2+} was similar in the two fibers, the peak amplitude of the Ca^{2+} signals was severely depressed at all voltages in the shPanx1 fiber. This was a reproducible feature as shown by the voltage-dependence of the mean values for peak rate of rise of fluo-4 Ca^{2+} transients in the two groups of fibers (Fig. 5B, n=17 (from 4 animals) and 21 (from 3 animals) control and shPanx1 fibers, respectively). Fitting a Boltzmann function to the peak rate values *versus* voltage in each fiber gave the mean parameters shown in the first row of the right panel in Fig. 5B. The comparison between the two sets of data was done using nested analysis and showed a significant 57 % reduction in the maximum rate of rise of fluo-4 fluorescence in

the shPanx1 fibers whereas the midpoint voltage and steepness factor were unchanged. The apparent time course of Ca^{2+} decay appeared unaffected in the shRNA-Panx1 fibers (Fig. 5A), suggesting that SERCA-mediated Ca^{2+} uptake was properly operating in this condition. To quantitatively appreciate the cytosolic Ca^{2+} removal capabilities of the fibers, we fitted a double exponential function to the decay of the Ca^{2+} transient after the end of the last depolarizing pulse of the protocol. The result from the fit is shown in blue superimposed to the traces in Fig. 5A. Mean values for the time constants did not differ between control and shRNA-Panx1 fibers but the final level was moderately but significantly depressed in the shPanx1 fibers (1.14 ± 0.04, as compared to 1.41 ± 0.07 in mCherry expressing fibers, n=17 (from 4 animals) and n=21 (from 3 animals) control and shPanx1 fibers, respectively).

As the reduced peak amplitude of voltage activated Ca^{2+} transients in shPanx1 muscle fibers may result from altered RyR1 activity or from the depressed driving force for the Ca^{2+} exit because of reduced SR content, we test whether the SR Ca^{2+} content differ between control and shPanx1 fibers. We used a protocol consisting in measuring the saturation level of the Ca^{2+}-sensitive dye indo-1 in fibers loaded with a high concentration of EGTA and challenged with repeated depolarizing pulses in the presence of cyclopiazonic acid (CPA), to release the SR Ca^{2+} content into the cytosol (see Methods). The left panel in Figure 5C shows the time course of resting indo-1 saturation level in a control and in a shPanx1 muscle fiber during that protocol. The right panel shows corresponding mean values obtained from 12 control fibers and 12 shPanx1 fibers muscle (N=3 animals), respectively. There was no significant difference between the two datasets. The SR Ca^{2+}

content was estimated in each fiber from the difference between the initial resting indo-1 saturation level before CPA application and the level reached at the end of the protocol, assuming 10 mM free EGTA was present in the intracellular medium and that EGTA and indo-1 have the same affinity for Ca^{2+}. This gave mean SR Ca^{2+} content values of 1.03 ± 0.13 and 1.24 ± 0.13 mM in control and shPanx1 fibers, respectively.

Intramembrane charge movement is not altered in fibers down expressing Pannexin-1.

We tested whether the changes in $Ca_V1.1$ function induced by reduced Panx1 expression were paralleled by changes in $Ca_V1.1$ voltage-sensor properties. For this, the intramembrane charge movement was compared between shPanx1 fibers and control fibers. Figure 6A shows representative traces of charge currents from a fiber of each group while Fig. 6B shows the mean voltage-dependence of the charge density from 11 (from 3 animals) and 16 control and shPanx1 fibers (from 3 animals), respectively. Fitting individual series of data points in each fiber with equation 2 gave mean values presented in Fig. 6C for the Boltzmann parameters. There was no difference in any parameter between control and shRNA-Panx1 fibers demonstrating that down-expression of Panx1 did not affect the $Ca_V1.1$ intramembrane charge movement and also demonstrating that the decreased Ca^{2+} channel conductance reported in Fig. 4 was not the consequence of reduced $Ca_V1.1$ expression level.

Discussion

$Ca_V1.1$ plays an essential role in skeletal muscle and its regulation by interaction

with partner proteins or protein complexes has shed light into the very exquisite manner it performs and regulates its functions. In the present work, we provide evidence for bidirectional functional interaction between $Ca_V1.1$ and Panx1. Control of Panx1 activity by $Ca_V1.1$ is involved in decoding the frequency of electrical activity and transducing it into transcriptional events crucial for muscle plasticity. In return, Panx1 now appears as a compulsory partner for proper function of $Ca_V1.1$ in EC coupling.

Role of Panx1 over Cav1.1: lessons from other Cav1.1 interacting proteins

We demonstrate here that reduced levels of Panx1 protein may alter some features of $Ca_V1.1$ function depressing activation of voltage-dependent SR Ca^{2+} release. Altered $Ca_V1.1$ activity was not due to a reduced amount of the $Ca_V1.1$ protein in the t-tubule membrane (as shown in Fig.6) as is the case, for instance, under conditions of down-expression of other proteins interacting with $Ca_V1.1$ and regulating its function (e.g. JP45 and junctophilin, (Golini et al. 2011, Yasuda et al. 2013)). Thus, changes in $Ca_V1.1$ activity in Ca^{2+} release must result from disruption of Panx1- $Ca_V1.1$ functional interaction and of proper organization and/or function of the $Ca_V1.1$-RyR1 interaction (EC coupling machinery), respectively. It is interesting to notice here, that there is not a simple correlation between change in $Ca_V1.1$ membrane content, changes in Ca^{2+} current and voltage-dependent SR Ca^{2+} release. For instance, in junctophilin1 deficient muscle cells, there is a reduction of about 60 % of peak amplitude of Ca^{2+} transients, without changes in Ca^{2+} currents or $Ca_V1.1$ membrane content (Nakada et al. 2018). Also, in muscle fibers from JP45/CASQ1 double KO mice, there is no significant change in $Ca_V1.1$ membrane content, but there is a robust increase of 45% in the Ca^{2+} conductance (Gmax) compared to

fibers from WT mice (Mosca et al. 2013). As proposed for other proteins, Panx1 could play a role in proper $Ca_V1.1$ tetrad formation. This is indeed a possibility as the functional phenotype combining reduction in $Ca_V1.1$ Ca^{2+} current and in SR Ca^{2+} release, together with preserved intramembrane charge movement, is reminiscent of what occurs either in the absence of RyR1(Nakai et al. 1996) or in the presence of a truncated form of the β_{1a} subunit of the DHPR (Eltit et al. 2014), both conditions being associated with disorganization of the standard arrangement of $Ca_V1.1$s in tetrad arrays (Eltit et al. 2014, Protasi et al. 1998). Accordingly, it may be that loss of Panx1 also contributes to disentangle the arrays to affect both orthograde and retrograde $Ca_V1.1$-RyR1 signaling.

From a more general point of view, we cannot exclude that the reduction of voltage-activated SR Ca^{2+} release associated with Panx1-knock-down, results from altered expression of one or several key proteins of the EC coupling machinery. Except from results from the charge movement experiments that limit the likelihood that the CaV1.1 expression level is affected, we cannot completely exclude that it is not the case for RyR1 or Stac3 or the β1 subunit of the DHPR or another critical component of the machinery.

Role of Cav1.1 over Panx1

We previously showed that $Ca_V1.1$ activates ATP release upon 20 Hz electrical stimulation in adult muscle fibers, leading to the activation of a signaling cascade related to muscle plasticity (Jorquera et al. 2013). Our present results demonstrate that, in addition to the control of $Ca_V1.1$ over Panx1, there is also a control of $Ca_V1.1$ by Panx1, through which Panx1 deficiency leads to dysfunction of $Ca_V1.1$ effect in EC coupling.

The functional interaction between $Ca_V1.1$ and Panx1 is important not only for

activation of Panx1 following electrical activity. Indeed, in resting conditions, the interaction also controls basal levels of ATP release. We previously reported that dysgenic myotubes (lacking $Ca_V1.1$), have increased levels of extracellular ATP release in basal conditions (Jorquera et al. 2013).We now show that in these cells the high level of ATP release is due to Panx1 activity (see Fig.1). Importantly, we also show that knock-down of $Ca_V1.1$ by a U7-exon skipping strategy in differentiated fibers also results in an increased resting level of ATP release and in altered expression of TnI isoforms. This suggests that, in these conditions, increased resting ATP release is sufficient to activate signaling pathways related to muscle plasticity in control muscle fibers.

The control of Panx1 by Cav1.1 in resting conditions is also important in some muscular disorders. In the mdx mouse model of Duchenne Muscular Dystrophy (DMD), there is a loss of negative control of ATP release in resting conditions (Valladares et al. 2013). The fact that the $Ca_V1.1$ blocker nifedipine improves the muscular function of mdx mice (Altamirano et al. 2013) highlights the importance of the above-mentioned interaction in this pathological muscle condition. Also, since there is evidence that Ca^{2+} release is depressed in mdx muscle fibers (Hollingworth et al. 2008, Woods et al. 2004), it could be speculated that this occurs, at least in part, because of the reduced interaction between $Ca_V1.1$ and Panx1. We expected that lack of Cav1.1 would have no effect or even decrease Panx1 activity; but experimentally, the reduction in Cav1.1 expression resulted in increased Panx1 activity, suggesting an inhibitory effect of $Ca_V1.1$ on Panx1-mediated permeation at rest.

Reduction in Panx1 decreased depolarization-induced Ca^{2+} release in the absence of SR Ca^{2+} depletion, suggesting that the lessening of Panx1 content could alter Cav1.1's

relationship with RyR1 in skeletal muscle fibers. Panx1 may be a good candidate to study in other models of dystrophies because the loss of Panx1 causes a deficient depolarization induced Ca^{2+} release that could contribute to muscle weakness present in several muscle pathologies (Jorquera et al., 2021). Altogether, $Ca_V1.1$-Panx1 interactions are essential for activation of gene transcription related to muscle plasticity, but they also may play an important role in certain muscle disorders, pointing to $Ca_V1.1$ as a potential target for the development of therapies.

Direct molecular interaction?

Even if the existence of a direct molecular interaction between Cav1.1 and Panx1 may be the simplest explanation for our results, we must be cautious in recognizing this interaction between $Ca_V1.1$ and Panx1 has not been fully demonstrated or molecularly mapped, although is suggested by the experimental evidence (co-immuno precipitation, co-localization using proximity ligation assay, co-migration in the same protein complex) described (Arias-Calderon et al. 2016, Jorquera et al. 2013). The present results suggest that the protein complex involved in excitation-contraction coupling (Cav1.1 and RyR1) also includes Panx1, as Panx1 and Cav1.1 have been identified, together with P2Y, to be part of the above-mentioned macromolecular complex (Arias-Calderon et al. 2016). Arias-Calderón et al. proposed that there are two different complexes along the T-tubule membrane; one near the surface membrane that includes (besides Cav1.1, Panx1 and P2Y2) caveolin3 and possibly dystrophin, and one that spans all the length of the T-tubule that includes P2Y2, Cav1.1 and which, according to the present results and its known location, should also include RyR1. The location of Panx1 was not clearly determined in the Arias-

Calderón et al. study, but upon a close look to the immunofluorescence images they show, Panx1 should also be considered in a complex that spans all the T-tubule length.

The apparent inhomogeneity of Panx1 along the T-tubule may be explained by the incapability of biochemical and localization assays to discriminate between immature and/or non-functional pool of proteins or by a lack of sensitivity of the antibodies to detect Panx1 in the center of the fiber. The effect we see on Ca^{2+} release could also be related to a non-linear release along the cross-section of the fiber, or to additional adaptive response mediated by signaling events provoked by the decrease in Panx1 as a secondary effect on the EC-coupling machinery.

Panx1 related disorders beyond the muscle

It is known that Panx1 channels are important in many organs. A case of a human autosomal recessive Panx1 missense gene variant exhibited intellectual disability and severe hearing loss, along with deficits in other organ systems including the skeleton (Shao et al. 2016). This gene variant consisted of an arginine to histidine substitution at position 217 (p.Arg217His) which was shown to reduce channel currents, dye flux, and ATP release while preserving surface expression. The severity of the impairments/disabilities observed are in apparent contradiction with the relatively modest phenotype in Panx1 KO mice. This modest phenotype has been speculated to be the result of compensation for the global loss of Panx1 from conception to adulthood. Indeed, evidence of compensation (by Panx3) in global Panx1 KO mice has been demonstrated (Lohman and Isakson 2014) (Whyte-Fagundes et al. 2018).

An interaction between Panx1 and other Ca_V channels has been suggested. $Ca_V1.2$

is present and functional in other tissues like lungs where it was found that Clevidipine, used to lower blood pressure, has an increased effect over $Ca_V1.2$ when Panx1 is present (Dahl et al. 2016). This may have an important clinical consequence because it would support the use of this dihydropyridine to reduce breathing problems and possibly also in the treatment of acute heart failure (Dahl et al. 2016). Thus, the functional interaction between Ca_V1 and Panx1 appears to be crucial not only for skeletal muscle but also for other tissues. Considering the widespread expression of Panx1 together with the presence of different members of the Ca_V family in heart, brain, and smooth muscle, we speculate that functional interaction between the two may be relevant in several physiological and pathological conditions.

Acknowledgements

We thank Jorge Hidalgo for his help in establishing and maintaining the electrophysiological set-up in Chile, and for helpful discussion and comments throughout the project. We thank Mónica Silva for providing isolated muscle fibers.

This work was supported by the Chilean-French cooperation program ECOS-Conicyt (#C13B01), by Fondecyt (grant #1151293 and postdoc # 3170194 to GJ), by Conicyt (fellowship #21130284 to J.T-G) and by grants from CNRS, INSERM, University Claude Bernard -Lyon 1 and the Association Française contre les Myopathies (AFM-Téléthon) to the Institut NeuroMyoGène.

Author contributions

Measurements of intramembrane charge movement (Fig. 6) and SR Ca^{2+} content (Fig. 5C) and of Ca^{2+} current and Ca^{2+} transients in muscle fibers down-expressing CaV1.1 (Fig. 2) were performed at Institut NeuroMyoGène, University Claude Bernard, Lyon 1. Measurements of DHPR protein level, ATP levels and gene expression in fibers down-expressing CaV1.1 (Fig. 1) were performed at Institut de Myologie, Université Paris 6. All other experiments were performed at the Muscle Physiology Laboratory, ICBM, University of Chile. Francisco Jaque, Gonzalo Jorquera, Mariana Casas (MC) and Vincent Jacquemond (VJ) performed experiments, analyzed results, and assembled figures. Jennifer Troc-Gajardo, Sonja Buvinic, and Bruno Allard performed experiments and analyzed results. Christel Gentil performed experiments, France Pietri-Rouxel contributed to design the experimental strategy, planned experiments, and analyzed results. Enrique Jaimovich

planned experiments, discussed results, and revised the manuscript. MC and VJ designed the project, planned the experiments, and wrote the manuscript. All authors approved the final version of the manuscript, agree to be accountable for all aspects of the work in ensuring that questions related to the accuracy or integrity of any part of the work are appropriately investigated and resolved. All persons designated as authors qualify for authorship, and all those who qualify for authorship are listed.

FIGURE LEGENDS

Figure 1. Leaky behavior of Pannexin-1 in adult muscle fibers down-expressing $Ca_V1.1$, mimics the effect induced by ATP after ES of fibers at 20 Hz. *A,* $Ca_V1.1$ down-expression by U7-exon skipping strategy (ΔDHPR fibers) induces a reduction of more than 60% in $Ca_V1.1$ protein level: the top panel shows a representative blot image while quantification of the reduction in Cav1.1 content is shown at the bottom (n=3 *fdb* muscles from 3 distinct mice). *B,* Extracellular ATP levels was measured in basal condition (CON) and after ES in WT and ΔDHPR fibers. We observed an increase by more than three times of the basal extracellular ATP level in ΔDHPR muscle fibers compared to WT ones. WT and ΔDHPR fibers received electrical stimulation (ES) consisted of 270 square pulses of 0.3 ms duration at 20 Hz. After ES WT fibers experienced a significant increase in extracellular ATP levels, meanwhile after ES, ΔDHPR fibers did not change extracellular ATP compared to CON condition (n=3 cultures from 3 distinct mice). *C,* A similar increase in basal extracellular ATP levels (CON) was observed in WT and lacking $Ca_V1.1$ (mdg) myotubes which was suppressed by incubation with 5μM of the Panx1 inhibitor Carbenoxolone (CBX) (n=5 independent experiments). *D,* Graph show that increased basal levels of mRNA for the slow isoform of TnI and decreased level for the fast isoform of TnI are observed in ΔDHPR *fdb* muscle fibers compared to WT fibers. 4h after ES, TnIs mRNA levels increased, while TnIf mRNA levels diminished in WT fibers. ΔDHPR fibers did not show changes in TnIs and TnIf mRNA levels after electrical stimulation (n=4 cultures from 4 distinct mice). Grey bars represent WT muscles and black bars represent ΔDHPR muscles. Significant differences within multiple groups were examined using Kruskal–Wallis test for repeated measures, followed by multiple comparison test. Mann-

Whitney test was used to detect significant differences between two groups. Data are expressed as mean ± SEM. */≠ $p<0.05$ and **/## $p<0.01$.

Figure 2. Reduced voltage-activated Ca^{2+} current and intracellular Ca^{2+} release in muscle fibers down-expressing $Ca_V1.1$

A, Ca^{2+} current records from a control fiber (left) and from a fiber down-expressing $Ca_V1.1$ (right). Currents were recorded in response to the voltage pulses shown on top. *B*, mean voltage-dependence of the peak $Ca_V1.1$ Ca^{2+} current density in control fibers and in fibers down-expressing $Ca_V1.1$. Graphs on the right show corresponding mean values for the current-voltage parameters obtained by fitting individual series of data points with equation 1. *C*, indo-1 Ca^{2+} transient elicited by a 20 ms-long depolarizing pulse to +10 mV in a control fiber and in a fiber down-expressing $Ca_V1.1$. Graphs on the right show corresponding mean values for resting and peak [Ca^{2+}] levels (results are from 14 control fibers and 14 fibers down-expressing $Ca_V1.1$from 4 mice). Black circles and bars correspond to control fibers and open circles and bars to fiber down-expressing $Ca_V1.1$. Data are expressed as mean ± SEM. Nested analysis was done for data of graph in B and C. *$p<0.05$ and ** $p<0.01$ vs control mCherry fibers.

Figure 3. Down expression of Panx1 decreases basal and post-ES (20 Hz) levels of extracellular ATP altering ES-dependent changes in gene expression. *A*, Panel showing red fluorescent fibers after 2 weeks of electroporation of *fdb* muscles with plasmid carrying mCherry (upper panel) and shPanx1-mCherry (lower panel). The corresponding transmitted light images demonstrate broad expression of both plasmids. *B*, Western blots

against Panx1 of *fdb* muscles shows that the muscles expressing the shRNA against Panx1 construct reduces Panx1 protein levels by ~65% (n=3 muscles from 3 distinct mice). *C*, the reduction of Panx1 in *fdb* fibers significantly decreases basal levels of extracellular ATP (left) as well as ES-activated ATP release (right) (n=5 culture plates from 5 distinct mice). *D*, 20 Hz ES-related changes in mRNA levels of TnIs and TnIf observed in mCherry fibers are suppressed in fiber knock down for Panx1 (n=3 distinct animals). We can observe a reduction of basal levels of TnIs mRNA in fibers knock down for Panx1 compared to control (98±5.5 in controls vs 54±15.7 in shPanx 1, but it reaches no statistical difference (p=0.1). Black bars represent mCherry expressing fibers and red bars represent shPanx1-mCherry expressing fibers. Significant differences within multiple groups were examined using Kruskal–Wallis test for repeated measures, followed by multiple comparison test. Mann-Whitney test was used to detect significant differences between two groups. Data are expressed as mean ± SEM. */≠ $p<0.05$ and ** $p<0.01$ vs control mCherry fibers.

Figure 4. Reduced expression of Pannexin-1 does not alter Ca^{2+} current through $Ca_V1.1$. *A*, Ca^{2+} current records from a control fiber (left) and from a fiber down-expressing Panx1 (right). Currents were recorded in response to the voltage pulses shown on top. *B*, mean voltage-dependence of the peak $Ca_V1.1$ Ca^{2+} current density in control fibers and in fibers down-expressing Panx1. *C*, the corresponding mean values for the current-voltage parameters obtained by fitting individual series of data points with equation 1. Mean values for the capacitance in the mCherry and in the shPanx1 groups of fibers used were 1.02 ± 0.14 and 1.22 ± 0.08 nF (n = 22 control fibers from 3 distinct mice and 21 fibers expressing the shRNA against Panx1 from 4 distinct mice). Black bars and lines

represent mCherry expressing fibers and red bars represent shPanx1-mCherry expressing fibers. Data are expressed as mean ± SEM. Nested analysis was done for data on C. *p<0.05 and ** p<0.01 vs control mCherry fibers.

Figure 5. Reduced expression of Pannexin-1 drastically alters voltage-activated SR Ca^{2+} release. *A,* fluo-4 F/F_0 Ca^{2+} transients recorded from a control fiber (left) and from a fiber down-expressing Panx1 (right). Transients were recorded in response to the voltage protocol shown on top. The superimposed blue line at the end of the record corresponds to the result from fitting a double-exponential plus constant function to the decay of the signal. *B,* voltage-dependence of the mean peak rate of rising of fluo-4 fluorescence in control fibers and in fibers down-expressing Panx1. Graphs in the upper row on the right show corresponding values for the Boltzmann parameters obtained from fitting individual series of data points with equation 2. Graphs in the bottom row on the right show mean values obtained from fitting the double exponential plus constant function to the final decay of the Fluo-4 transient. *C,* estimation of the SR Ca^{2+} content: indo-1 resting saturation level was measured in control fibers and in fibers down-expressing Panx1 challenged by repeated depolarizing pulses in the presence of CPA. An example of the corresponding time course of change in indo-1 saturation in a fiber of each group is shown on the left. Mean values are shown on the right (n=12 fibers for both control and shPanx1 muscles from 3 distinct mice). Black bars and lines represent mCherry expressing fibers and red bars and lines represent shPanx1-mCherry expressing fibers.. Data are expressed as mean ± SEM. */≠ p<0.05. Nested analysis was performed in data from graphs shown in B.

Figure 6. Expression of shRNA against Pannexin-1 does not alter intramembrane

charge movements in fibers down expressing Pannexin-1. *A*, illustrative traces of intramembrane charge current in a control fiber (left) and in a fiber down-expressing Panx1 (right). *B*, the voltage dependence of the mean amount of charge in control fibers and in fibers down-expressing Panx1. The inset shows the good equality between *on* and *off* charge. *C*, mean values for the parameters obtained from fitting a Boltzmann function to the individual series of data points (n=12 fibers for both control and shPanx1 muscles from 4 distinct mice). Black bars and lines represent mCherry expressing fibers and red bars and lines represent shPanx1-mCherry expressing fibers. Data are expressed as mean ± SEM.

Altamirano, F., Valladares, D., Henriquez-Olguin, C., Casas, M., Lopez, J. R., Allen, P. D. and Jaimovich, E. (2013). "Nifedipine treatment reduces resting calcium concentration, oxidative and apoptotic gene expression, and improves muscle function in dystrophic mdx mice." PLoS One **8**(12): e81222.

Anderson, A. A., Altafaj, X., Zheng, Z., Wang, Z. M., Delbono, O., Ronjat, M., Treves, S. and Zorzato, F. (2006). "The junctional SR protein JP-45 affects the functional expression of the voltage-dependent Ca2+ channel Cav1.1." J Cell Sci **119**(Pt 10): 2145-2155.

Andronache, Z., Hamilton, S. L., Dirksen, R. T. and Melzer, W. (2009). "A retrograde signal from RyR1 alters DHP receptor inactivation and limits window Ca2+ release in muscle fibers of Y522S RyR1 knock-in mice." Proc Natl Acad Sci U S A **106**(11): 4531-4536.

Arias-Calderon, M., Almarza, G., Diaz-Vegas, A., Contreras-Ferrat, A., Valladares, D., Casas, M., Toledo, H., Jaimovich, E. and Buvinic, S. (2016). "Characterization of a multiprotein complex involved in excitation-transcription coupling of skeletal muscle." Skelet Muscle **6**: 15.

Bannister, R. A. and Beam, K. G. (2009). "Ryanodine modification of RyR1 retrogradely affects L-type Ca(2+) channel gating in skeletal muscle." J Muscle Res Cell Motil **30**(5-6): 217-223.

Bao, L., Locovei, S. and Dahl, G. (2004). "Pannexin membrane channels are mechanosensitive conduits for ATP." FEBS Lett **572**(1-3): 65-68.

Baranova, A., Ivanov, D., Petrash, N., Pestova, A., Skoblov, M., Kelmanson, I., Shagin, D., Nazarenko, S., Geraymovych, E., Litvin, O., Tiunova, A., Born, T. L., Usman, N., Staroverov, D., Lukyanov, S. and Panchin, Y. (2004). "The mammalian pannexin family is homologous to the invertebrate innexin gap junction proteins." Genomics **83**(4): 706-716.

Beam, K. G. and Bannister, R. A. (2010). "Looking for answers to EC coupling's persistent questions." J Gen Physiol **136**(1): 7-12.

Buvinic, S., Almarza, G., Bustamante, M., Casas, M., Lopez, J., Riquelme, M., Saez, J. C., Huidobro-Toro, J. P. and Jaimovich, E. (2009). "ATP released by electrical stimuli elicits calcium transients and gene expression in skeletal muscle." J Biol Chem **284**(50): 34490-34505.

Casas, M., Buvinic, S. and Jaimovich, E. (2014). "ATP signaling in skeletal muscle: from fiber plasticity to regulation of metabolism." Exerc Sport Sci Rev **42**(3): 110-116.

Casas, M., Figueroa, R., Jorquera, G., Escobar, M., Molgo, J. and Jaimovich, E. (2010). "IP(3)-dependent, post-tetanic calcium transients induced by electrostimulation of adult skeletal muscle fibers." J Gen Physiol **136**(4): 455-467.

Collet, C., Csernoch, L. and Jacquemond, V. (2003). "Intramembrane charge movement and L-type calcium current in skeletal muscle fibers isolated from control and mdx mice." Biophys J **84**(1): 251-265.

Corriden, R. and Insel, P. A. (2010). "Basal release of ATP: an autocrine-paracrine mechanism for cell regulation." Sci Signal **3**(104): re1.

Couchoux, H., Allard, B., Legrand, C., Jacquemond, V. and Berthier, C. (2007). "Loss of caveolin-3 induced by the dystrophy-associated P104L mutation impairs L-type calcium channel function in mouse skeletal muscle cells." J Physiol **580**(Pt.3): 745-754.

Chekeni, F. B., Elliott, M. R., Sandilos, J. K., Walk, S. F., Kinchen, J. M., Lazarowski, E. R., Armstrong, A. J., Penuela, S., Laird, D. W., Salvesen, G. S., Isakson, B. E., Bayliss, D. A. and Ravichandran, K. S. (2010). "Pannexin 1 channels mediate 'find-me' signal release and membrane permeability during apoptosis." Nature **467**(7317): 863-867.

D'Hondt, C., Ponsaerts, R., De Smedt, H., Vinken, M., De Vuyst, E., De Bock, M., Wang, N., Rogiers, V., Leybaert, L., Himpens, B. and Bultynck, G. (2011). "Pannexin channels in ATP release and beyond: an unexpected rendezvous at the endoplasmic reticulum." Cell Signal **23**(2): 305-316.
Dahl, G. P., Conner, G. E., Qiu, F., Wang, J., Spindler, E., Campagna, J. A. and Larsson, H. P. (2016). "High affinity complexes of pannexin channels and L-type calcium channel splice-variants in human lung: Possible role in clevidipine-induced dyspnea relief in acute heart failure." EBioMedicine **10**: 291-297.
Dayal, A., Schrotter, K., Pan, Y., Fohr, K., Melzer, W. and Grabner, M. (2017). "The Ca(2+) influx through the mammalian skeletal muscle dihydropyridine receptor is irrelevant for muscle performance." Nat Commun **8**(1): 475.
Eltit, J. M., Franzini-Armstrong, C. and Perez, C. F. (2014). "Amino acid residues 489-503 of dihydropyridine receptor (DHPR) beta1a subunit are critical for structural communication between the skeletal muscle DHPR complex and type 1 ryanodine receptor." J Biol Chem **289**(52): 36116-36124.
Esteve, E., Eltit, J. M., Bannister, R. A., Liu, K., Pessah, I. N., Beam, K. G., Allen, P. D. and Lopez, J. R. (2010). "A malignant hyperthermia-inducing mutation in RYR1 (R163C): alterations in Ca2+ entry, release, and retrograde signaling to the DHPR." J Gen Physiol **135**(6): 619-628.
Gallot, Y. S., McMillan, J. D., Xiong, G., Bohnert, K. R., Straughn, A. R., Hill, B. G. and Kumar, A. (2017). "Distinct roles of TRAF6 and TAK1 in the regulation of adipocyte survival, thermogenesis program, and high-fat diet-induced obesity." Oncotarget **8**(68): 112565-112583.
Georgiou, D. K., Dagnino-Acosta, A., Lee, C. S., Griffin, D. M., Wang, H., Lagor, W. R., Pautler, R. G., Dirksen, R. T. and Hamilton, S. L. (2015). "Ca2+ Binding/Permeation via Calcium Channel, CaV1.1, Regulates the Intracellular Distribution of the Fatty Acid Transport Protein, CD36, and Fatty Acid Metabolism." J Biol Chem **290**(39): 23751-23765.
Golini, L., Chouabe, C., Berthier, C., Cusimano, V., Fornaro, M., Bonvallet, R., Formoso, L., Giacomello, E., Jacquemond, V. and Sorrentino, V. (2011). "Junctophilin 1 and 2 proteins interact with the L-type Ca2+ channel dihydropyridine receptors (DHPRs) in skeletal muscle." J Biol Chem **286**(51): 43717-43725.
Hollingworth, S., Zeiger, U. and Baylor, S. M. (2008). "Comparison of the myoplasmic calcium transient elicited by an action potential in intact fibres of mdx and normal mice." J Physiol **586**(21): 5063-5075.
Horowicz, P. and Schneider, M. F. (1981). "Membrane charge moved at contraction thresholds in skeletal muscle fibres." J Physiol **314**: 595-633.
Hu, H., Wang, Z., Wei, R., Fan, G., Wang, Q., Zhang, K. and Yin, C. C. (2015). "The molecular architecture of dihydropyrindine receptor/L-type Ca2+ channel complex." Sci Rep **5**: 8370.
Jacquemond, V. (1997). "Indo-1 fluorescence signals elicited by membrane depolarization in enzymatically isolated mouse skeletal muscle fibers." Biophys J **73**(2): 920-928.
Jorquera, G., Altamirano, F., Contreras-Ferrat, A., Almarza, G., Buvinic, S., Jacquemond, V., Jaimovich, E. and Casas, M. (2013). "Cav1.1 controls frequency-dependent events regulating adult skeletal muscle plasticity." J Cell Sci **126**(Pt 5): 1189-1198.
Lee, C. S., Dagnino-Acosta, A., Yarotskyy, V., Hanna, A., Lyfenko, A., Knoblauch, M., Georgiou, D. K., Poche, R. A., Swank, M. W., Long, C., Ismailov, II, Lanner, J., Tran, T., Dong, K., Rodney, G. G., Dickinson, M. E., Beeton, C., Zhang, P., Dirksen, R. T. and Hamilton, S. L. (2015). "Ca(2+) permeation and/or binding to CaV1.1 fine-tunes skeletal muscle Ca(2+) signaling to sustain muscle function." Skelet Muscle **5**: 4.
Legrand, C., Giacomello, E., Berthier, C., Allard, B., Sorrentino, V. and Jacquemond, V. (2008). "Spontaneous and voltage-activated Ca2+ release in adult mouse skeletal muscle fibres expressing the type 3 ryanodine receptor." J Physiol **586**(2): 441-457.

Locovei, S., Wang, J. and Dahl, G. (2006). "Activation of pannexin 1 channels by ATP through P2Y receptors and by cytoplasmic calcium." FEBS Lett **580**(1): 239-244.
Lohman, A. W. and Isakson, B. E. (2014). "Differentiating connexin hemichannels and pannexin channels in cellular ATP release." FEBS Lett **588**(8): 1379-1388.
Melhorn, M. I., Brodsky, A. S., Estanislau, J., Khoory, J. A., Illigens, B., Hamachi, I., Kurishita, Y., Fraser, A. D., Nicholson-Weller, A., Dolmatova, E., Duffy, H. S. and Ghiran, I. C. (2013). "CR1-mediated ATP release by human red blood cells promotes CR1 clustering and modulates the immune transfer process." J Biol Chem **288**(43): 31139-31153.
Mormeneo, E., Jimenez-Mallebrera, C., Palomer, X., De Nigris, V., Vazquez-Carrera, M., Orozco, A., Nascimento, A., Colomer, J., Lerin, C. and Gomez-Foix, A. M. (2012). "PGC-1alpha induces mitochondrial and myokine transcriptional programs and lipid droplet and glycogen accumulation in cultured human skeletal muscle cells." PLoS One **7**(1): e29985.
Mosca, B., Delbono, O., Laura Messi, M., Bergamelli, L., Wang, Z. M., Vukcevic, M., Lopez, R., Treves, S., Nishi, M., Takeshima, H., Paolini, C., Martini, M., Rispoli, G., Protasi, F. and Zorzato, F. (2013). "Enhanced dihydropyridine receptor calcium channel activity restores muscle strength in JP45/CASQ1 double knockout mice." Nat Commun **4**: 1541.
Nakada, T., Kashihara, T., Komatsu, M., Kojima, K., Takeshita, T. and Yamada, M. (2018). "Physical interaction of junctophilin and the CaV1.1 C terminus is crucial for skeletal muscle contraction." Proc Natl Acad Sci U S A **115**(17): 4507-4512.
Nakai, J., Dirksen, R. T., Nguyen, H. T., Pessah, I. N., Beam, K. G. and Allen, P. D. (1996). "Enhanced dihydropyridine receptor channel activity in the presence of ryanodine receptor." Nature **380**(6569): 72-75.
Nishida, M., Sato, Y., Uemura, A., Narita, Y., Tozaki-Saitoh, H., Nakaya, M., Ide, T., Suzuki, K., Inoue, K., Nagao, T. and Kurose, H. (2008). "P2Y6 receptor-Galpha12/13 signalling in cardiomyocytes triggers pressure overload-induced cardiac fibrosis." EMBO J **27**(23): 3104-3115.
Paolini, C., Fessenden, J. D., Pessah, I. N. and Franzini-Armstrong, C. (2004). "Evidence for conformational coupling between two calcium channels." Proc Natl Acad Sci U S A **101**(34): 12748-12752.
Pelegrin, P. and Surprenant, A. (2006). "Pannexin-1 mediates large pore formation and interleukin-1beta release by the ATP-gated P2X7 receptor." EMBO J **25**(21): 5071-5082.
Perni, S., Lavorato, M. and Beam, K. G. (2017). "De novo reconstitution reveals the proteins required for skeletal muscle voltage-induced Ca(2+) release." Proc Natl Acad Sci U S A **114**(52): 13822-13827.
Pietri-Rouxel, F., Gentil, C., Vassilopoulos, S., Baas, D., Mouisel, E., Ferry, A., Vignaud, A., Hourde, C., Marty, I., Schaeffer, L., Voit, T. and Garcia, L. (2010). "DHPR alpha1S subunit controls skeletal muscle mass and morphogenesis." EMBO J **29**(3): 643-654.
Polster, A., Nelson, B. R., Olson, E. N. and Beam, K. G. (2016). "Stac3 has a direct role in skeletal muscle-type excitation-contraction coupling that is disrupted by a myopathy-causing mutation." Proc Natl Acad Sci U S A **113**(39): 10986-10991.
Pouvreau, S., Allard, B., Berthier, C. and Jacquemond, V. (2004). "Control of intracellular calcium in the presence of nitric oxide donors in isolated skeletal muscle fibres from mouse." J Physiol **560**(Pt 3): 779-794.
Protasi, F., Franzini-Armstrong, C. and Allen, P. D. (1998). "Role of ryanodine receptors in the assembly of calcium release units in skeletal muscle." J Cell Biol **140**(4): 831-842.
Rebbeck, R. T., Karunasekara, Y., Board, P. G., Beard, N. A., Casarotto, M. G. and Dulhunty, A. F. (2014). "Skeletal muscle excitation-contraction coupling: who are the dancing partners?" Int J Biochem Cell Biol **48**: 28-38.

Rios, E. and Brum, G. (1987). "Involvement of dihydropyridine receptors in excitation-contraction coupling in skeletal muscle." Nature **325**(6106): 717-720.
Rios, E. and Pizarro, G. (1991). "Voltage sensor of excitation-contraction coupling in skeletal muscle." Physiol Rev **71**(3): 849-908.
Robin, G. and Allard, B. (2015). "Voltage-gated Ca(2+) influx through L-type channels contributes to sarcoplasmic reticulum Ca(2+) loading in skeletal muscle." J Physiol **593**(21): 4781-4797.
Romanov, R. A., Rogachevskaja, O. A., Bystrova, M. F., Jiang, P., Margolskee, R. F. and Kolesnikov, S. S. (2007). "Afferent neurotransmission mediated by hemichannels in mammalian taste cells." EMBO J **26**(3): 657-667.
Samso, M. (2015). "3D Structure of the Dihydropyridine Receptor of Skeletal Muscle." Eur J Transl Myol **25**(1): 4840.
Schneider, M. F. (1994). "Control of calcium release in functioning skeletal muscle fibers." Annu Rev Physiol **56**: 463-484.
Shao, Q., Lindstrom, K., Shi, R., Kelly, J., Schroeder, A., Juusola, J., Levine, K. L., Esseltine, J. L., Penuela, S., Jackson, M. F. and Laird, D. W. (2016). "A Germline Variant in the PANX1 Gene Has Reduced Channel Function and Is Associated with Multisystem Dysfunction." J Biol Chem **291**(24): 12432-12443.
Silverman, W. R., de Rivero Vaccari, J. P., Locovei, S., Qiu, F., Carlsson, S. K., Scemes, E., Keane, R. W. and Dahl, G. (2009). "The pannexin 1 channel activates the inflammasome in neurons and astrocytes." J Biol Chem **284**(27): 18143-18151.
Sridharan, M., Adderley, S. P., Bowles, E. A., Egan, T. M., Stephenson, A. H., Ellsworth, M. L. and Sprague, R. S. (2010). "Pannexin 1 is the conduit for low oxygen tension-induced ATP release from human erythrocytes." Am J Physiol Heart Circ Physiol **299**(4): H1146-1152.
Tanabe, T., Beam, K. G., Adams, B. A., Niidome, T. and Numa, S. (1990). "Regions of the skeletal muscle dihydropyridine receptor critical for excitation-contraction coupling." Nature **346**(6284): 567-569.
Thompson, R. J., Jackson, M. F., Olah, M. E., Rungta, R. L., Hines, D. J., Beazely, M. A., MacDonald, J. F. and MacVicar, B. A. (2008). "Activation of pannexin-1 hemichannels augments aberrant bursting in the hippocampus." Science **322**(5907): 1555-1559.
Thompson, R. J., Zhou, N. and MacVicar, B. A. (2006). "Ischemia opens neuronal gap junction hemichannels." Science **312**(5775): 924-927.
Valladares, D., Almarza, G., Contreras, A., Pavez, M., Buvinic, S., Jaimovich, E. and Casas, M. (2013). "Electrical stimuli are anti-apoptotic in skeletal muscle via extracellular ATP. Alteration of this signal in Mdx mice is a likely cause of dystrophy." PLoS One **8**(11): e75340.
Weiss, N., Couchoux, H., Legrand, C., Berthier, C., Allard, B. and Jacquemond, V. (2008). "Expression of the muscular dystrophy-associated caveolin-3(P104L) mutant in adult mouse skeletal muscle specifically alters the Ca(2+) channel function of the dihydropyridine receptor." Pflugers Arch **457**(2): 361-375.
Weiss, N., Legrand, C., Pouvreau, S., Bichraoui, H., Allard, B., Zamponi, G. W., De Waard, M. and Jacquemond, V. (2010). "In vivo expression of G-protein beta1gamma2 dimer in adult mouse skeletal muscle alters L-type calcium current and excitation-contraction coupling." J Physiol **588**(Pt 15): 2945-2960.
Whyte-Fagundes, P., Kurtenbach, S., Zoidl, C., Shestopalov, V. I., Carlen, P. L. and Zoidl, G. (2018). "A Potential Compensatory Role of Panx3 in the VNO of a Panx1 Knock Out Mouse Model." Front Mol Neurosci **11**: 135.
Woods, C. E., Novo, D., DiFranco, M. and Vergara, J. L. (2004). "The action potential-evoked sarcoplasmic reticulum calcium release is impaired in mdx mouse muscle fibres." J Physiol **557**(Pt 1): 59-75.

Yasuda, T., Delbono, O., Wang, Z. M., Messi, M. L., Girard, T., Urwyler, A., Treves, S. and Zorzato, F. (2013). "JP-45/JSRP1 variants affect skeletal muscle excitation-contraction coupling by decreasing the sensitivity of the dihydropyridine receptor." Hum Mutat **34**(1): 184-190.

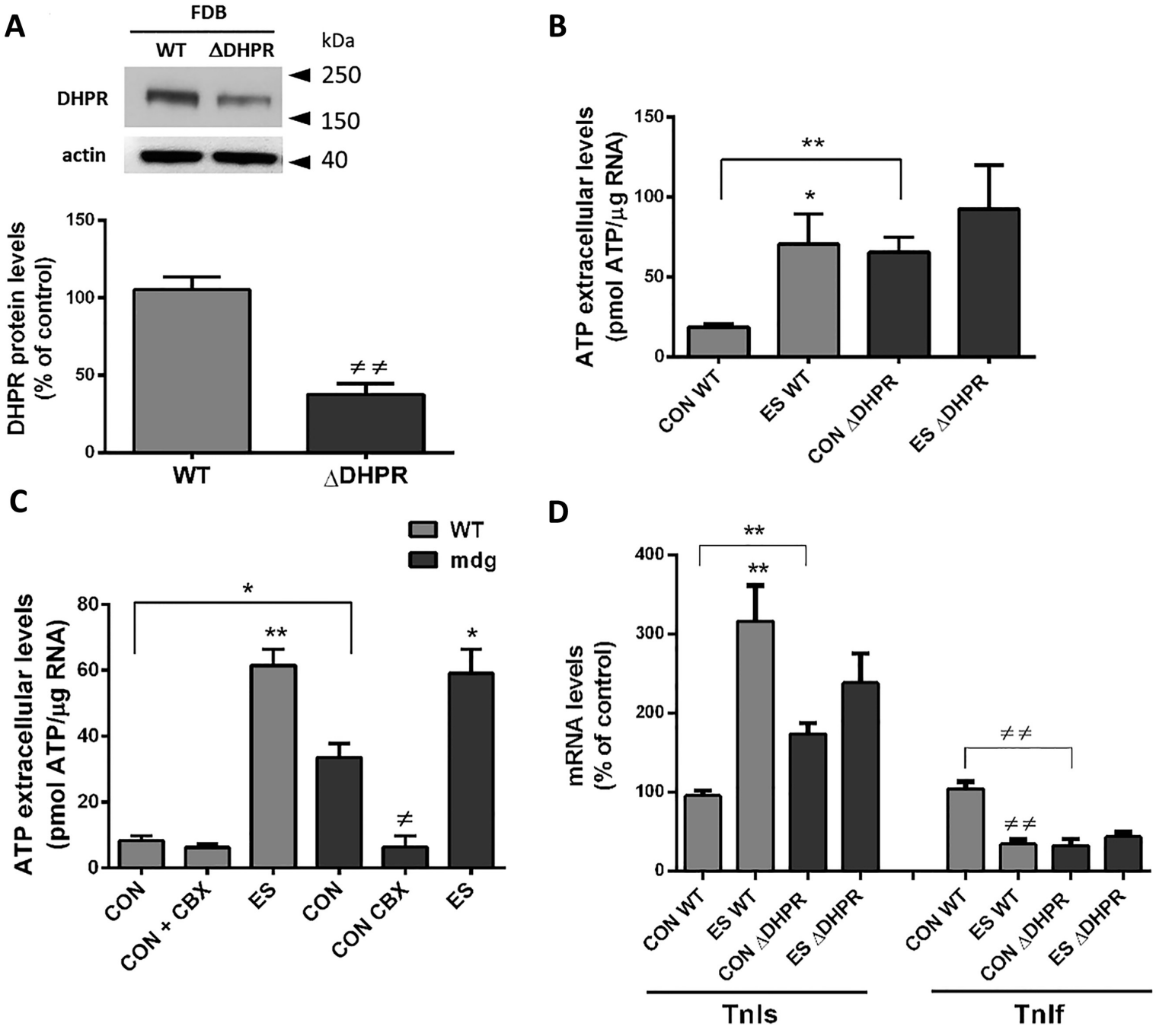
A
FDB
WT
ΔDHPR
kDa
DHPR
actin
250
150
40
DHPR protein levels (% of control)
150
100
50
0
≠≠
WT
ΔDHPR
B
ATP extracellular levels (pmol ATP/μg RNA)
150
100
50
0
**
*
CON WT
ES WT
CON ΔDHPR
ES ΔDHPR
C
WT
mdg
ATP extracellular levels (pmol ATP/μg RNA)
80
60
40
20
0
*
**
*
≠
CON
CON + CBX
ES
CON
CON CBX
ES
D
mRNA levels (% of control)
400
300
200
100
0
**
**
≠≠
≠≠
CON WT
ES WT
CON ΔDHPR
ES ΔDHPR
CON WT
ES WT
CON ΔDHPR
ES ΔDHPR
TnIs
TnIf

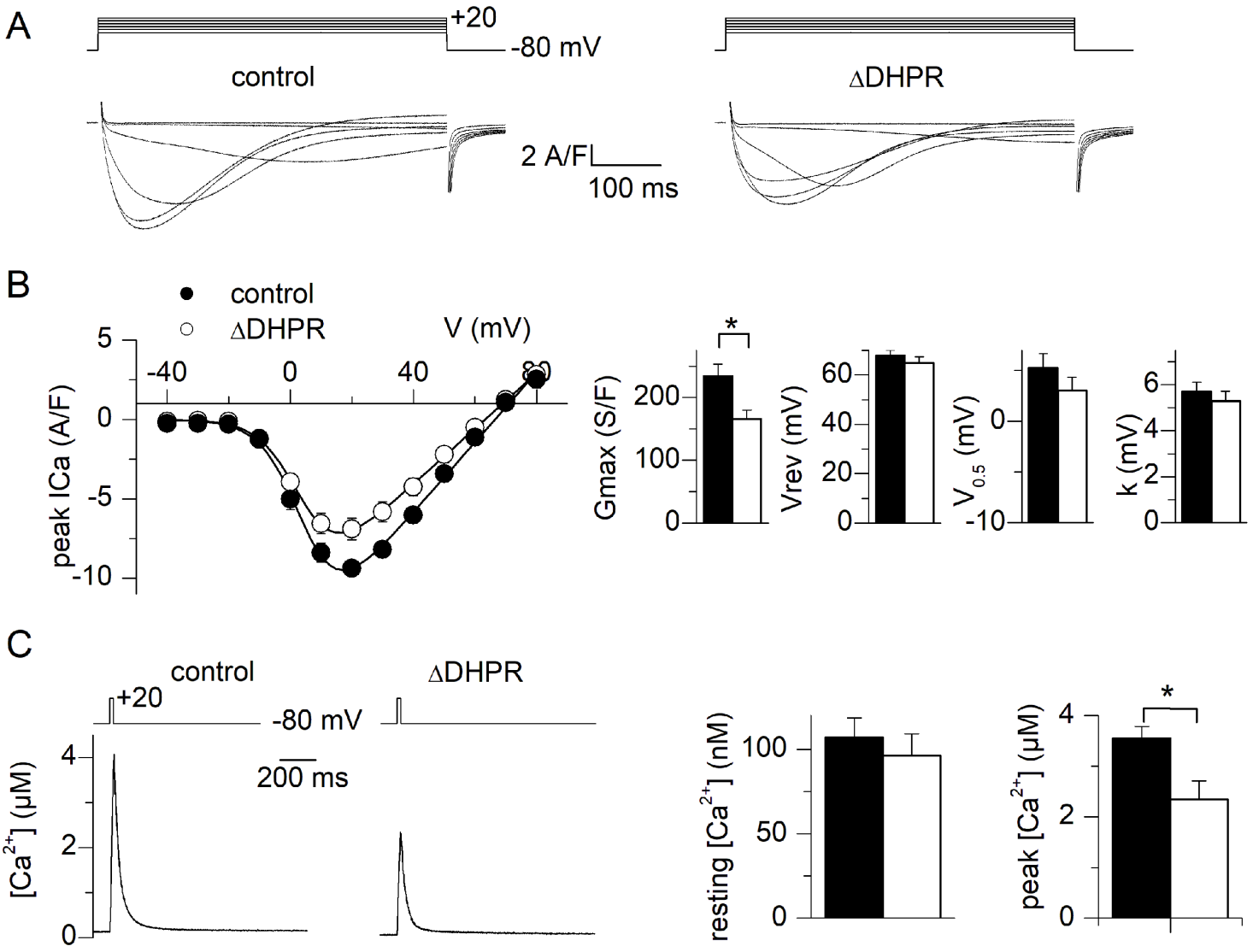
A
+20
-80 mV
control
ΔDHPR
2 A/F
100 ms
B
control
ΔDHPR
V (mV)
peak ICa (A/F)
5
0
-5
-10
-40
0
40
80
Gmax (S/F)
200
100
0
*
Vrev (mV)
60
40
20
0
V0.5 (mV)
0
-10
k (mV)
6
4
2
0
C
control
ΔDHPR
+20
-80 mV
200 ms
[Ca2+] (μM)
4
2
0
resting [Ca2+] (nM)
100
50
0
peak [Ca2+] (μM)
4
2
0
*

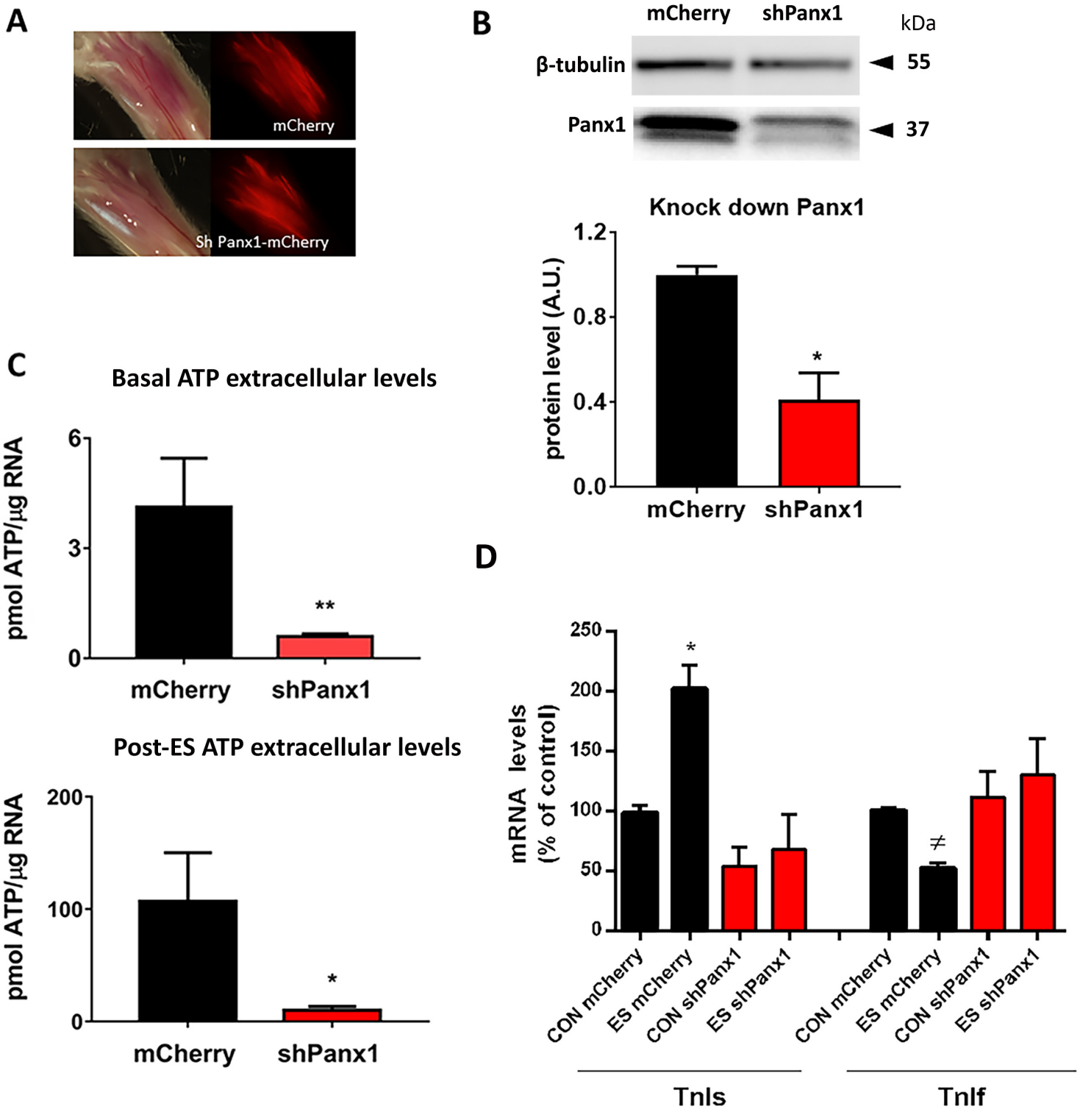
A
mCherry
Sh Panx1-mCherry
B
mCherry
shPanx1
kDa
β-tubulin
55
Panx1
37
Knock down Panx1
protein level (A.U.)
1.2
0.8
0.4
0.0
*
mCherry
shPanx1
C
Basal ATP extracellular levels
pmol ATP/µg RNA
6
3
0
**
mCherry
shPanx1
Post-ES ATP extracellular levels
pmol ATP/µg RNA
200
100
0
*
mCherry
shPanx1
D
mRNA levels
(% of control)
250
200
150
100
50
0
*
≠
CON mCherry
ES mCherry
CON shPanx1
ES shPanx1
CON mCherry
ES mCherry
CON shPanx1
ES shPanx1
TnIs
TnIf

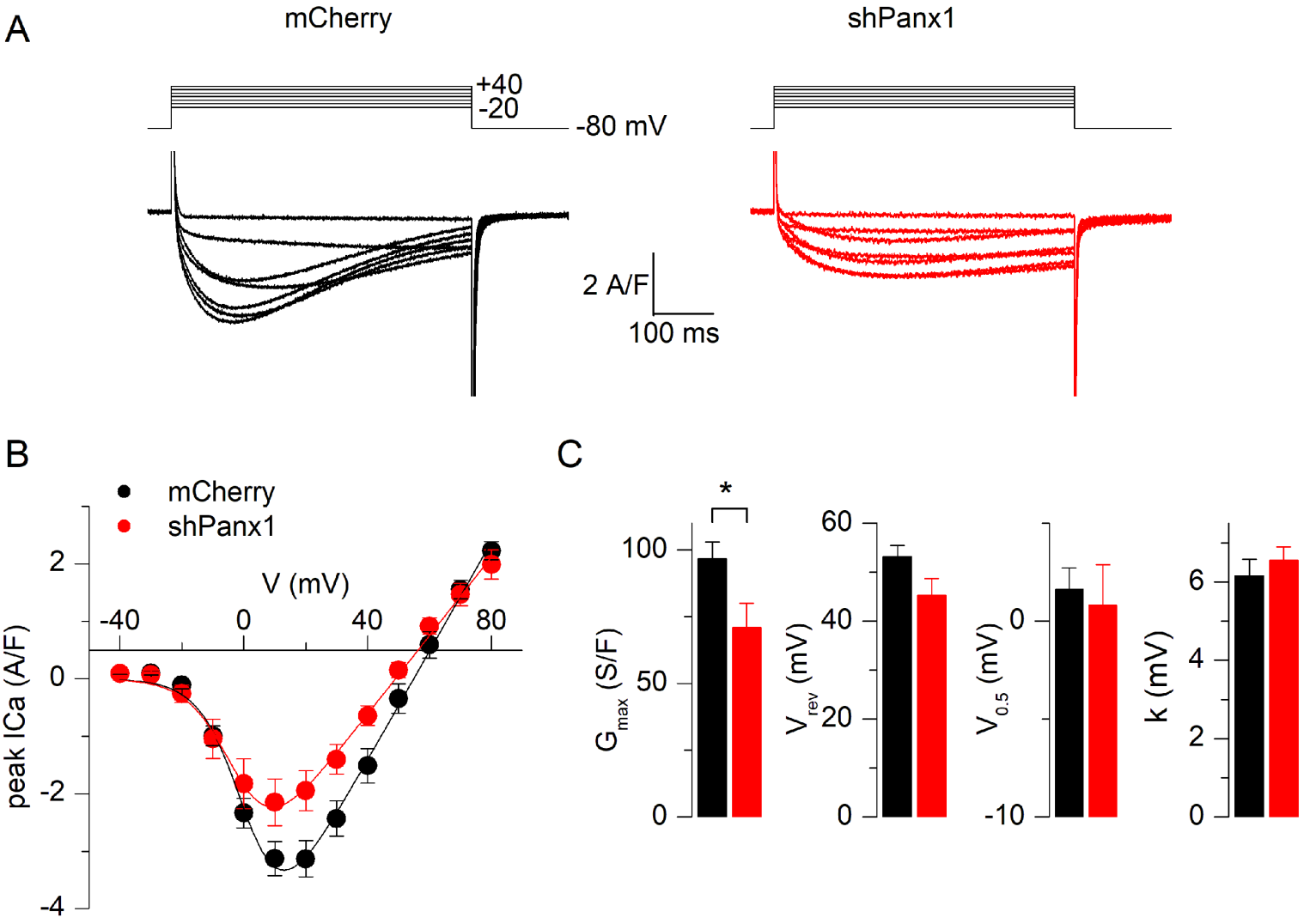
A
mCherry
shPanx1
+40
-20
-80 mV
2 A/F
100 ms
B
mCherry
shPanx1
V (mV)
-40
0
40
80
peak ICa (A/F)
2
0
-2
-4
C
*
100
50
0
G_max (S/F)
60
40
20
0
V_rev (mV)
0
-10
V_0.5 (mV)
6
4
2
0
k (mV)

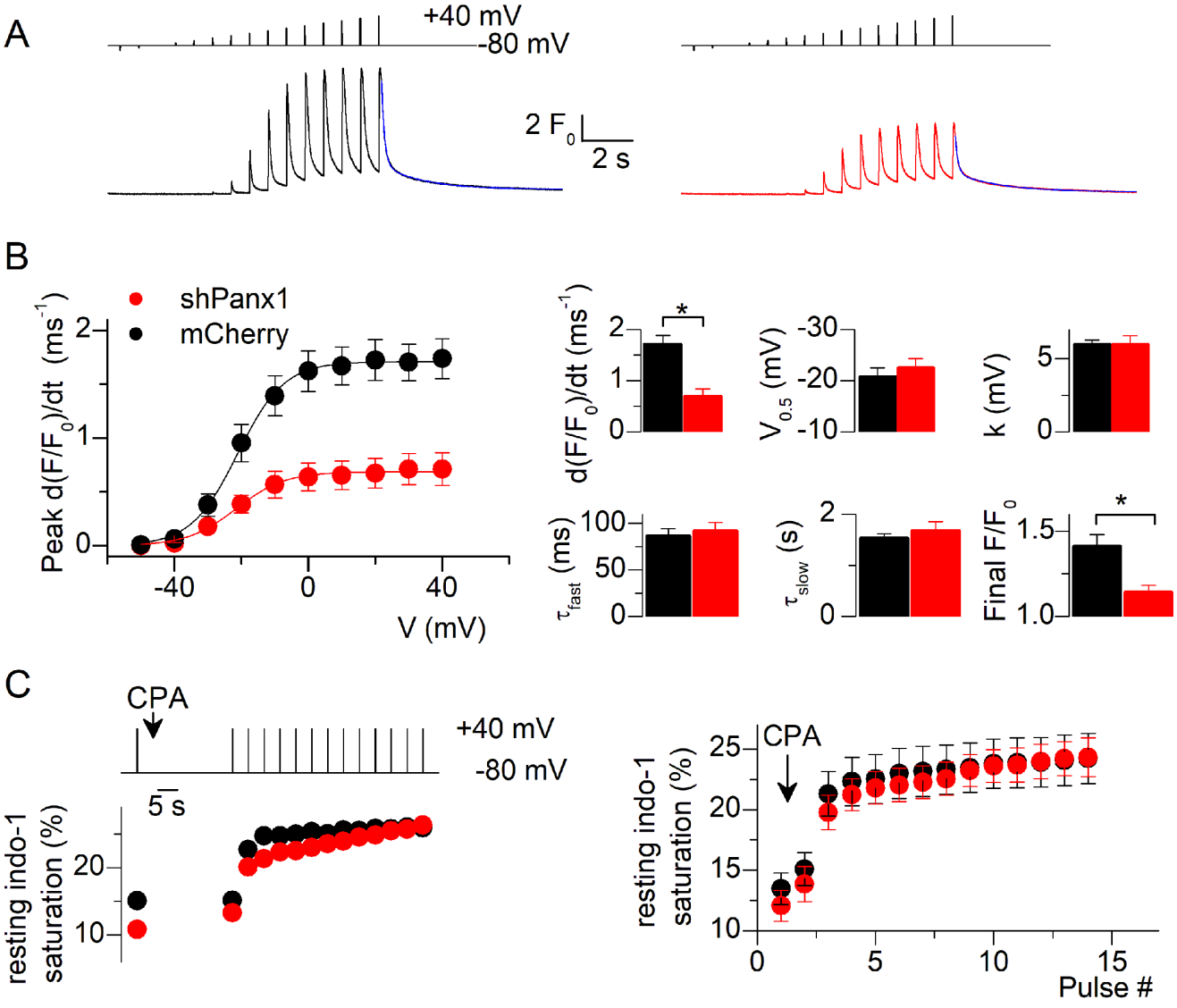
A
+40 mV
-80 mV
2 F0
2 s
B
shPanx1
mCherry
Peak d(F/F0)/dt (ms-1)
V (mV)
d(F/F0)/dt (ms-1)
V0.5 (mV)
k (mV)
τfast (ms)
τslow (s)
Final F/F0
C
CPA
+40 mV
-80 mV
5 s
resting indo-1 saturation (%)
Pulse #

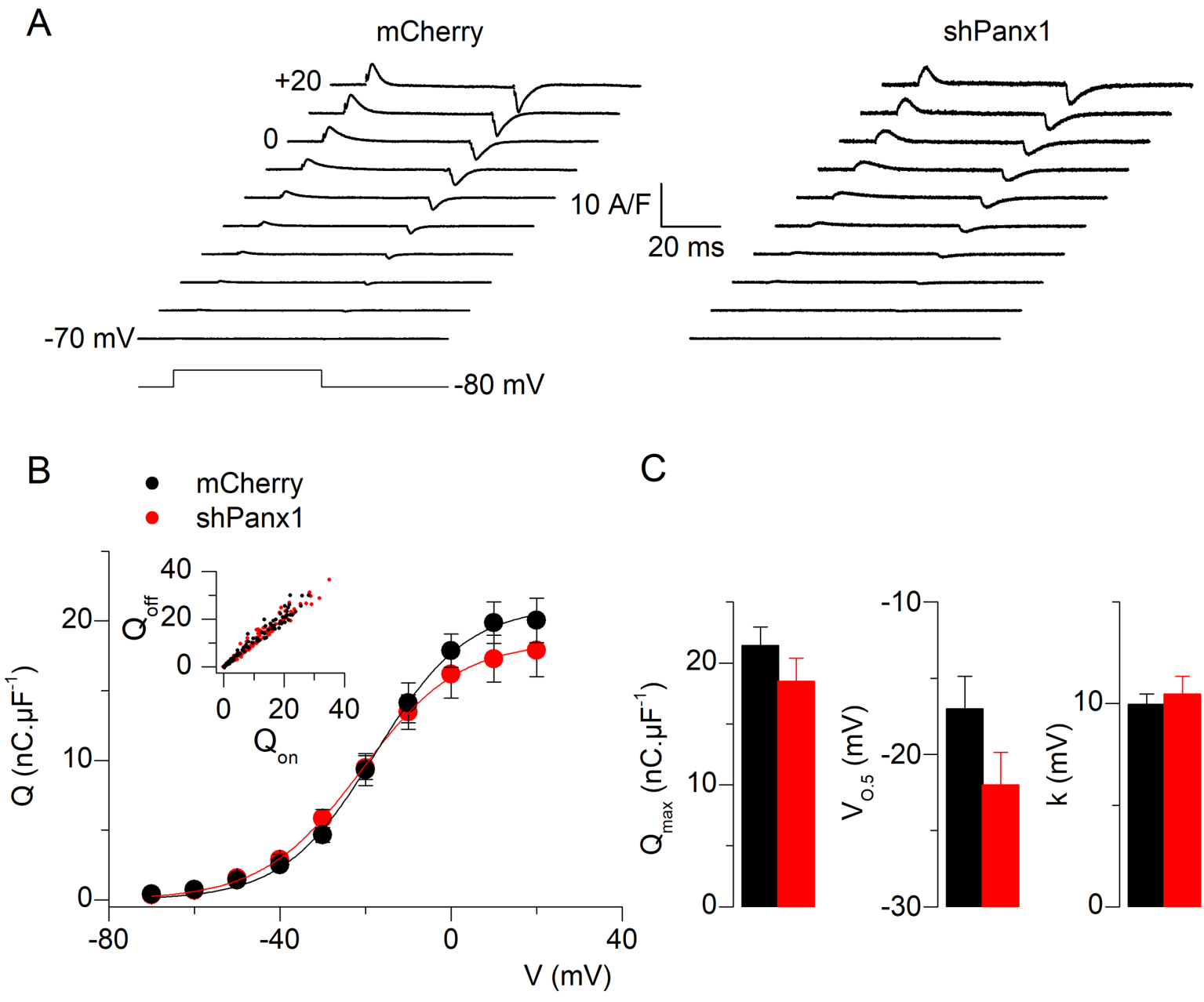
A
mCherry
shPanx1
+20
0
10 A/F
20 ms
-70 mV
-80 mV
B
mCherry
shPanx1
Q (nC.µF-1)
Qoff
Qon
V (mV)
C
Qmax (nC.µF-1)
VO.5 (mV)
k (mV)